AAC Journals.ASM.org

Antagonism between Bacteriostatic and Bactericidal Antibiotics Is Prevalent

Paolo S. Ocampo,[a,c] Viktória Lázár,[b] Balázs Papp,[b] Markus Arnoldini,[c,d] Pia Abel zur Wiesch,[e] Róbert Busa-Fekete,[f] Gergely Fekete,[b] Csaba Pál,[b] Martin Ackermann,[c,d] Sebastian Bonhoeffer[a]

Institute of Integrative Biology, ETH Zürich, Zürich, Switzerland[a]; Synthetic and Systems Biology Unit, Biological Research Centre, Hungarian Academy of Sciences, Szeged, Hungary[b]; Department of Environmental Microbiology, Eawag, Dübendorf, Switzerland[c]; Institute of Biogeochemistry and Pollutant Dynamics, ETH Zürich, Zürich, Switzerland[d]; Division of Global Health Equity, Brigham and Women's Hospital/Harvard Medical School, Boston, Massachusetts, USA[e]; Linear Accelerator Laboratory, University of Paris-Sud, CNRS, Orsay, France[f]

Combination therapy is rarely used to counter the evolution of resistance in bacterial infections. Expansion of the use of combination therapy requires knowledge of how drugs interact at inhibitory concentrations. More than 50 years ago, it was noted that, if bactericidal drugs are most potent with actively dividing cells, then the inhibition of growth induced by a bacteriostatic drug should result in an overall reduction of efficacy when the drug is used in combination with a bactericidal drug. Our goal here was to investigate this hypothesis systematically. We first constructed time-kill curves using five different antibiotics at clinically relevant concentrations, and we observed antagonism between bactericidal and bacteriostatic drugs. We extended our investigation by performing a screen of pairwise combinations of 21 different antibiotics at subinhibitory concentrations, and we found that strong antagonistic interactions were enriched significantly among combinations of bacteriostatic and bactericidal drugs. Finally, since our hypothesis relies on phenotypic effects produced by different drug classes, we recreated these experiments in a microfluidic device and performed time-lapse microscopy to directly observe and quantify the growth and division of individual cells with controlled antibiotic concentrations. While our single-cell observations supported the antagonism between bacteriostatic and bactericidal drugs, they revealed an unexpected variety of cellular responses to antagonistic drug combinations, suggesting that multiple mechanisms underlie the interactions.

The problem of antibiotic resistance requires a solution that relies on more than just the development of new drugs. Pathogens have been unrelenting in evolving mechanisms by which to survive in the face of every drug put on the market. Combination therapy, i.e., the concurrent application of two or more antibiotics, provides an appealing approach that demands closer assessment as a tool to combat this problem. In the treatment of important infectious diseases such as HIV infection, tuberculosis, and malaria, combination therapy has become the standard approach precisely to delay the evolution of drug resistance (1–4). In contrast, for common acute bacterial infections, combinations of drugs are prescribed in only a very limited number of cases and with a different rationale (5). In those specific instances, two drugs are prescribed for their synergistic effects, that is, for the fact that their combined effects exceed the sum of their individual effects. Drug synergy has been demonstrated to result in more-efficient clearance of infections and to achieve clearance at lower drug concentrations (6). Examples of such cases include fusidic acid and rifampin for the treatment of methicillin-resistant *Staphylococcus aureus* infections and trimethoprim and sulfamethoxazole for the treatment of otitis media (7, 8). Furthermore, recent theoretical work indicates that synergistic drugs can prevent treatment failure even when bacteria resistant to one of the drugs are present at the beginning of therapy (9).

Just as synergy can be exploited to improve treatment, it is necessary to avoid combinations of drugs that inhibit each other and may prolong infections. Antagonism, when a drug hinders the effect of another drug, was reported early in the history of antibiotics and continues to function as a warning against indeterminate treatment (10). In a study of patients with pneumococcal meningitis, 30% of those treated with penicillin alone failed treatment and died, while 79% of comparable patients who were treated with the same dosage of penicillin plus chlortetracycline, an antibiotic that antagonizes penicillin, died (11, 12).

Despite these findings, an increasing number of laboratory studies indicate that antagonistic drug combinations merit more investigation as clinical options (13). Recent work in this area suggests that the different types of interactions have significant effects on the selection and maintenance of drug resistance mutations. Using a direct competition experiment, Chait and colleagues demonstrated how a hyperantagonistic drug combination was able to select against a bacterial population resistant to one of the drugs and instead favored the completely sensitive wild type (14). Furthermore, the rate of adaptation of laboratory bacteria to multiple drugs has been shown to correlate with the degree of synergism between individual antibiotics (15). Although antagonistic drug combinations are currently eschewed in clinical settings, these studies suggest that antagonism between antibiotics may aid in devising treatment strategies specifically aimed at delaying the emergence of resistance.

Received 5 February 2014 **Returned for modification** 15 April 2014
Accepted 21 May 2014
Published ahead of print 27 May 2014
Address correspondence to Paolo S. Ocampo, paolosocampo@gmail.com.
C. Pál, M. Ackermann, and S. Bonhoeffer contributed equally to this article.
Supplemental material for this article may be found at http://dx.doi.org/10.1128/AAC.02463-14.

doi:10.1128/AAC.02463-14

TABLE 1 List of all antibiotics used in the study

Abbreviation	Antibiotic	EC_{90}[a] (μg/ml)	Main mechanism of action	Bactericidal/bacteriostatic status
AMP	Ampicillin	1.2	Cell wall	Bactericidal
PIP	Piperacillin	1.5	Cell wall	Bactericidal
FOX	Cefoxitin	1.4	Cell wall	Bactericidal
FOS	Fosfomycin	14	Cell wall	Bactericidal
LOM	Lomefloxacin	0.12	Gyrase	Bactericidal
CPR	Ciprofloxacin	0.0055	Gyrase	Bactericidal
NAL	Nalidixic acid	2.3	Gyrase	Bactericidal
FSM	Fosmidomycin	40	Lipid	Bactericidal
NIT	Nitrofurantoin	2.4	Multiple mechanisms	Bactericidal
AMK	Amikacin	3.4	Aminoglycoside, 30S protein synthesis	Bactericidal
GEN	Gentamicin	0.66	Aminoglycoside, 30S protein synthesis	Bactericidal
KAN	Kanamycin	3	Aminoglycoside, 30S protein synthesis	Bactericidal
TOB	Tobramycin	0.85	Aminoglycoside, 30S protein synthesis	Bactericidal
STR	Streptomycin	4.5	Aminoglycoside, 30S protein synthesis	Bactericidal
TET	Tetracycline	0.3	30S protein synthesis	Bacteriostatic
DOX	Doxycycline	0.23	30S protein synthesis	Bacteriostatic
CHL	Chloramphenicol	1	50S protein synthesis	Bacteriostatic
ERY	Erythromycin	8.5	50S protein synthesis	Bacteriostatic
FUS	Fusidic acid	200	50S protein synthesis	Bacteriostatic
SLF	Sulfamonomethoxine	1.9	Folic acid biosynthesis	Bacteriostatic
TRM	Trimethoprim	0.4	Folic acid biosynthesis	Bacteriostatic

[a] EC_{90} represents the concentration of an antibiotic at which 90% of the maximal growth inhibitory effect was observed.

In response to the slow development of new antimicrobials, there is renewed interest in old drugs that have fallen out of use due to toxicity or drawbacks in efficacy (16). One approach that could be implemented to return these drugs to the clinic is to use an old drug in combination with a current drug (17). The advantages of synergism and the diverse nontrivial effects of antagonism will play a central role in determining how best to implement combination therapy in clinical settings.

In order to exploit the potential benefits of combination therapy, we need a better understanding of the circumstances under which synergism versus antagonism is expected. Determining how a broader spectrum of drugs interact at inhibitory concentrations and delineating the mechanisms responsible for these effects could allow for a more-prudent application of antibiotics that maintains clinical capability and does not sacrifice the future utility of these drugs.

In this study, we asked whether basic pharmacodynamic properties of all antibiotics can help predict which pairs would result in antagonism. A widely recognized characteristic of antibiotics is that they are either bacteriostatic and inhibit growth without killing the cells or are bactericidal and result in cell killing (18). Thus, if bactericidal drugs are most potent with actively growing cells, as hypothesized more than 50 years ago (19, 20), then the inhibition of growth induced by a bacteriostatic drug should result in a reduction of drug efficacy. To test this hypothesis, we determined the types of interaction between five different drugs at inhibitory concentrations by estimating death rates using time-kill curves. We then extended our observations and employed screening methods to identify effects across pairs of 21 different drugs at subinhibitory concentrations. Since our hypothesis relies on the decreased antibiotic susceptibility of slowly growing cells and the ability of some drugs to influence this state, we repeated our experiments at the level of individual cells using time-lapse microscopy, in microfluidic devices, to investigate the cellular dynamics underlying combined effects of antibiotics.

MATERIALS AND METHODS

High-throughput combination screening experiments. We selected 21 antibiotics with a wide range of mechanisms of action, including drugs that target cell wall, nucleic acid, protein, and folic acid biosynthesis (Table 1). Fresh antibiotic solutions were prepared from powder stocks on a weekly basis and were filter sterilized before use. All experiments were conducted in *Escherichia coli* K-12 (BW25113) in minimal medium supplemented with 0.2% glucose and 0.1% Casamino Acids. Combination screens were performed in 384-well plates, using a liquid-handling robotic system (Hamilton Star workstation) to improve reproducibility. The culture volume was 50 μl. Each plate contained two different 6-by-6 dose-matrix blocks (one antibiotic in combination with two other antibiotics), with 4 replicates each. For each pair of antibiotics, we combined 6 different concentrations of the agents in a serially diluted two-dimensional dose matrix, with dose points being centered on the 50% effective concentration (EC_{50}) for each antibiotic. The lowest concentration for each agent was 0 and the highest was above the 90% effective concentration (EC_{90}) (Table 1). In addition to the dose-matrix blocks, each plate included 18 wells containing medium without antibiotics (control wells).

Antibiotic sensitivity screens were performed by growing cells overnight (optical density at 600 nm [OD_{600}], 4) at 30°C, with shaking at 300 rpm, and diluting the cells to an OD equivalent to 0.04. Next, using a liquid-handling robotic system, cells were transferred into 384-well assay plates (in the presence of antibiotics) to yield 4×10^4 cells/well. Assay plates were incubated for 18 h at 30°C, with shaking at 300 rpm. Bacterial growth was monitored by measuring the optical density (OD_{600}) of the liquid cultures at a single time point. Preliminary experiments showed that a single reading of optical density after 18 h of incubation showed strong linear correlation with the area under the growth curve (a descriptor of overall inhibitory effect that covers the entire growth period) (21). Briefly, this was determined using parallel cultures of *E. coli* grown in ten 384-well microtiter plates under previously stated conditions. Optical density (OD_{600}) was measured every hour for 24 h, and the areas under the growth curves were determined using custom MATLAB scripts. For a number of different ending time points (e.g., 11, 12, and 13 h), we used a linear regression model to consider whether the last OD measurements predicted the areas under the growth curves ($384 \times 10 = 3{,}840$ data points). Plates were prepared as multiple (up to 6) biological replicates,

and those with quality control problems (e.g., growth in control wells was unusually low or showed large variations or an agent failed to substantially inhibit growth at high concentrations or strongly inhibited growth at even low doses) were omitted from further analysis.

We had two reasons to study antibiotic interactions in a standard minimal medium at a relatively low temperature (30°C). First, because the culture volume in our study was 50 μl, evaporation was a potential concern. To minimize such a confounding effect, 30°C appeared to be an optimal solution. Second, our experimental setting was similar to that of a prior study (22), allowing direct comparison of the results of the two studies.

Data processing and bias correction steps. To overcome any measurement bias caused by within-plate inhomogeneity, we processed the raw optical density data as follows. We included 18 control wells on each plate, containing medium without antibiotics and inoculated with *E. coli*. We used these wells both to set a baseline for zero inhibition and to estimate and to eliminate within-plate systematic biases. First we calibrated OD values by applying the transformation $OD_{calibrated} = OD + (0.40449 \times OD^3)$, to account for the nonlinear association between OD and cell density at high cell densities (parameters of the calibration formula were derived as in reference 23). Then we calculated relative inhibition values based on the initial OD (maximum inhibition) and the average OD of antibiotic-free control wells (maximum growth). To estimate and to eliminate within-plate spatial effects, first we fitted a linear trend to the control wells to eliminate spatial gradients. Next, for the residuals, we employed Gaussian process regression (24) to eliminate the remaining systematic spatial biases using the control wells. Both steps for bias correction were carried out in MATLAB.

Identification of interacting antibiotic pairs. Synergistic effects between combinations of chemicals, resulting in increased benefits or increased toxicity, have important implications across the fields of biomedicine (25, 26). Correspondingly, many approaches have been devised to quantify drug interactions (27). To assess antagonism and synergy between pairs of antibiotics, we used the Loewe additivity model (28), which assumes that a drug does not interact with itself. Geometrically, Loewe additivity can be represented as lines of equally effective dosages (isoboles) in the two-dimensional linear concentration space for the two drugs. Deviation of the shape of the isoboles from linearity indicates either synergy (concave isoboles) or antagonism (convex isoboles). To identify interactions for each pair of antibiotics, first we merged data from replicate dose-matrix blocks located on the same 384-well plates. Next we fitted sigmoidal dose-response curves (Hill equation) to the single-agent responses using a maximum likelihood fitting procedure. Based on the single-agent response curves for the two antibiotics, we calculated the dose-response relationship for the antibiotic combination expected with the Loewe additivity model. To quantify interactions, we determined the concavity of the set of isoboles inferred from the combination measurements for a given antibiotic pair ("observed" isoboles). To achieve this, we used a mathematical transformation to "bend" the linear isoboles expected under the Loewe additivity model to approximate most closely the observed isoboles (see the report by Cokol and colleagues for a similar approach [29]). The transformation relies on a single parameter to describe the concavity of the observed isoboles, which we used as a measure of antibiotic interaction. This score is zero in the absence of interaction, negative for antagonistic pairs, and positive for synergistic pairs. Finally, interaction scores (B) for each antibiotic pair were calculated by taking the median scores obtained from biological replicates (i.e., independent plates).

Measurement errors of interaction screens were estimated by testing 5 antibiotics for interactions with themselves in multiple replicates (29). Because under Loewe additivity a drug shows no interaction with itself, deviation of the interaction score from zero provides an estimate of the experimental error of interaction measurements. Thus, we considered two antibiotics as significantly interacting when the score was significantly different from the mean score for self-self antibiotic combinations. For calculation of EC_{50} values, we followed established protocols (30). EC_{50} refers to the concentration of drug that induces growth inhibition halfway between the baseline and maximum values after the specified exposure time.

Antibiotics and concentrations for time-kill and time-lapse microscopy experiments. Determination of the clinical utility of exploiting different interactions between pairs of antibiotics will require extensive testing across organisms, sites of infection, and the drugs used for particular infections. In contrast, we consider our work a proof-of-principle study, and future work should confirm potential clinical implications. Although some of the antibiotics we used have advanced derivatives in the clinic, the choice of the drugs we used was based on two criteria, i.e., (i) the availability of very detailed literature on the molecular mechanism of action and (ii) the possibility for comparison with the results of an older study (22). Similarly, the antibiotic concentrations used do not reflect clinical recommendations. For example, although the concentration of erythromycin used in our time-kill and time-lapse microscopy experiments is higher than that achievable in blood, this drug was included to illustrate the effect of antagonism between a drug at an inhibitory concentration and a second drug at a subinhibitory concentration. Although the MIC for erythromycin in *E. coli* MG1655 is well above the concentration we used (500 to 1,000 μg/ml), we were interested in determining whether a subinhibitory concentration of this drug was sufficient to antagonize the killing effect of a second drug whose concentration was above the MIC.

Time-kill curves. Determination of the MICs for the antibiotics used in the time-kill and time-lapse microscopy studies was carried out using a broth dilution protocol similar to that recommended by the Clinical and Laboratory Standards Institute (LB medium was used instead of Mueller-Hinton broth) (31). The concentrations of the drugs used in the following experiments represent fractions of the MICs: 25 μg/ml streptomycin and nalidixic acid (2× MIC), 12.5 μg/ml tetracycline (0.83× MIC), 10 μg/ml trimethoprim, (0.66× MIC), and 200 μg/ml erythromycin (0.4× MIC).

Overnight cultures of *E. coli* MG1655 were diluted 1:10,000 into fresh prewarmed LB broth and were incubated for 2 h. A further 1:2 dilution was performed before introduction into flasks containing either a single antibiotic or a pair of bactericidal and bacteriostatic antibiotics. These were then incubated at 37°C with shaking and aeration. Samples were taken at 1-h intervals for up to 5 h. Cell densities for each sample were estimated from colony counts by dilution in phosphate-buffered saline and plating on LB agar. Each time-kill experiment was performed twice.

Time-lapse microscopy. Specific details of the microfluidic system used in this study, the mother machine, have been described previously (32). In brief, this device consists of 4,000 growth channels arranged at right angles against a large trench, through which growth medium is passed. Nutrients then diffuse into the channels and flush out growing cells as they emerge from these channels. An automated microscope stage allows for the monitoring of multiple fields of view, spanning the entire device. This method results in the continuous observation of the growth and division of a large number of individual cells as they experience different antibiotic-containing environments, as well as their survival or death after the drug has been removed.

Time-lapse microscopy experiments were conducted as follows. *E. coli* MG1655 cultures were grown overnight in LB broth at 37°C. On the following day, 100 μl of culture was diluted in 10 ml of fresh prewarmed LB broth and then was incubated for 2 h at 37°C, with shaking. Eight milliliters of the resulting culture was centrifuged at 10,000 rpm for 5 to 7 min and resuspended in 20 μl of fresh LB broth; 10 μl of the cell suspension was then injected into the mother machine, and the experiment was initiated when more than 80% of the channels were filled with cells via diffusion. A syringe pump was used to pass fresh LB broth supplemented with bovine serum albumin (BSA) and salmon sperm DNA through the device at a rate of 2 ml/h. BSA and salmon sperm DNA are blocking agents that are used to bind to the surface of the microfluidic device to prevent the formation of air bubbles and excessive adhesion of the cells to the channels. Images were acquired from 15 to 25 fields of view at 6-min intervals by using an automated Olympus BX81 microscope with an

UPLFN100×O2PH/1.3 phase-contrast oil lens. Samples and the microscope were held at 37°C with a cube-and-box incubation system (Life Imaging Services, Reinach, Switzerland). After at least 4 h of growth in LB broth, the medium was switched to LB broth containing BSA, salmon sperm, and either one or two antibiotics. Cells were exposed to this medium for at least 20 h before being switched back to fresh LB broth supplemented with BSA and salmon sperm DNA for up to 10 h. Each experiment involved fields scanned continuously for at least 30 h.

The resulting time-lapse images were then analyzed with a custom-designed plug-in for ImageJ, to provide information on cell size and division rates during the three different phases of the experiment. The first step of the analysis consists of defining the length of the cell abutting the end of the channel. The increasing length of the growing cell over succeeding frames is tracked and recorded; division events are also registered based on cell length. Manual verification and annotation were performed after every experiment. In this way, we were able to extract quantitative information on an individual cell's elongation and division rates. We also tracked the proportion of cells that survived treatment exposure and were able to divide again upon the return to an antibiotic-free environment. The occurrence of filamentation during exposure to the antibiotics erythromycin and nalidixic acid led to elongated cells being pulled out of their growth channels during flow. For this reason, only channels containing cells that could be followed for the entirety of the experiment were considered in the analysis.

RESULTS

Time-kill curves. To quantify interactions between antibiotics at clinically relevant concentrations, we measured death rates at inhibitory drug levels based on time-kill curves. We tested every possible bactericidal-bacteriostatic pair among five antibiotics at concentrations above the MIC. The antibiotics used in the time-kill experiments were selected for their differing mechanisms of action and because, to the best of our knowledge, there are no reports of cross-resistance mutations for these drugs in *E. coli*.

In the presence of a bactericidal drug that alone is capable of clearing a bacterial population, the addition of a bacteriostatic drug resulted in a decrease in killing rates and a significant number of survivors at the end of the experiment (Fig. 1). We also noted that the degree of antagonism differed depending on the bactericidal drug employed in the experiment. Acquisition of a resistance mutation over the course of the time-kill curve experiment could be a confounding effect explaining the reduced death rate observed in bacterial cultures treated with a bactericidal-bacteriostatic pair. In order to control for this possibility, the colonies obtained at the end of every time-kill curve experiment were replica plated on antibiotic-containing plates. We found no evidence for the evolution of single-drug or multidrug resistance in any replicate, to any of the drugs used in the experiment (data not shown). These time-kill curves provide confirmation that the antagonistic interactions found between drugs at inhibitory concentrations manifest as decreases in the rate of killing and the presence of significant proportions of sensitive bacteria at the end of the experiment.

Systematic exploration of interactions between bactericidal and bacteriostatic antibiotics. We expanded our observations of interactions between drugs to a total of 21 antibacterial compounds. These antibiotics cover a wide range of mechanisms of action, and many of them are widely employed clinically. Their main targets include DNA synthesis, translational machinery, and cell wall, folic acid, and lipid biosynthesis (Table 1). We systematically measured the effects of all pairs of antibiotics on *E. coli* K-12 growth rates. Specifically, for each pair of antibiotics, we combined 6 different concentrations of the agents in a two-dimensional dose matrix, with dose points being centered on each antibiotic's half-maximal effective concentration (EC_{50}). We used the Loewe additivity model to assess interactions between antibiotics (33). In contrast to other models, this model measures drug-drug interactions based on deviation from a drug-with-itself reference. According to the Loewe additivity model, if the modes of action of two drugs are the same, then the drugs show no interaction. Lines of equal effective dosages (isoboles) are represented in the two-dimensional linear concentration space of the two drugs. Deviation of these lines from a linear model indicates synergism (concave) or antagonism (convex). We introduced several correction steps to overcome potential measurement biases due to plate inhomogeneity, and we also developed a rigorous statistical framework to assess the significance of interactions. Following a previously developed method, we quantified isobole shapes by measuring concavity (using B interaction scores), where $B = 0$ indicates independent effects of the two drugs (linearity) and $B < 0$ and $B > 0$ indicate antagonism and synergism, respectively (see Materials and Methods). In this work, we focus on studying the properties of antagonistic antibiotic pairs only; synergism will be studied elsewhere.

Using a statistical criterion to identify significant interactions (see Materials and Methods), we found that 61% of the 204 antibiotic pairs showed antagonism. The reliability of our results was confirmed by comparison with a previous systematic drug combination screen performed in *E. coli* (22). Despite the substantial differences in the protocols and the underlying assumptions of the models used in the two studies, interaction scores were well correlated (Spearman's rho, 0.529; $P < 0.0001$) and antagonistic pairs identified in the previous study tended to have especially low scores in our screen (Mann-Whitney U test, $P < 0.0001$). Furthermore, our high-throughput survey correctly identified a well-characterized antagonism between ciprofloxacin and tetracycline (34).

The distribution of antagonism is highly nonrandom on the map of interactions. We compared the B scores for antibiotic interactions in two groups, i.e., antibiotic pairs that target the same and different cellular subsystems. The comparison revealed that B scores were especially low for antibiotic pairs targeting different cellular subsystems (Mann-Whitney U test, $P < 0.0001$). In line with the expectations of the Loewe model, antibiotic pairs targeting the same cellular subsystem rarely showed strong antagonism.

More strikingly, combinations of 30S protein synthesis and cell wall biosynthesis inhibitors, 50S protein synthesis and gyrase inhibitors, and cell wall biosynthesis and folic acid synthesis inhibitors frequently showed antagonism ($P < 0.05$ for each combination, Fisher's exact test). A common property of these combinations is that a bacteriostatic compound is combined with a bactericidal agent. To minimize the chance of erroneous classification, we used only *E. coli*-specific information for bactericidal/bacteriostatic classifications (Table 1). To test more generally whether antagonism was enriched in bacteriostatic-bactericidal combinations, we categorized antibiotic pairs according to individual antibiotic killing properties, which led to three major groups, namely, bactericidal-bactericidal, bactericidal-bacteriostatic, and bacteriostatic-bacteriostatic pairs. Strikingly, we found that antibiotic pairs with exceptionally low B interaction scores, denoting a high degree of antagonism, were nearly always bactericidal-bacteriostatic ($P = 0.0016$, Fisher's exact test) (Fig. 2). This

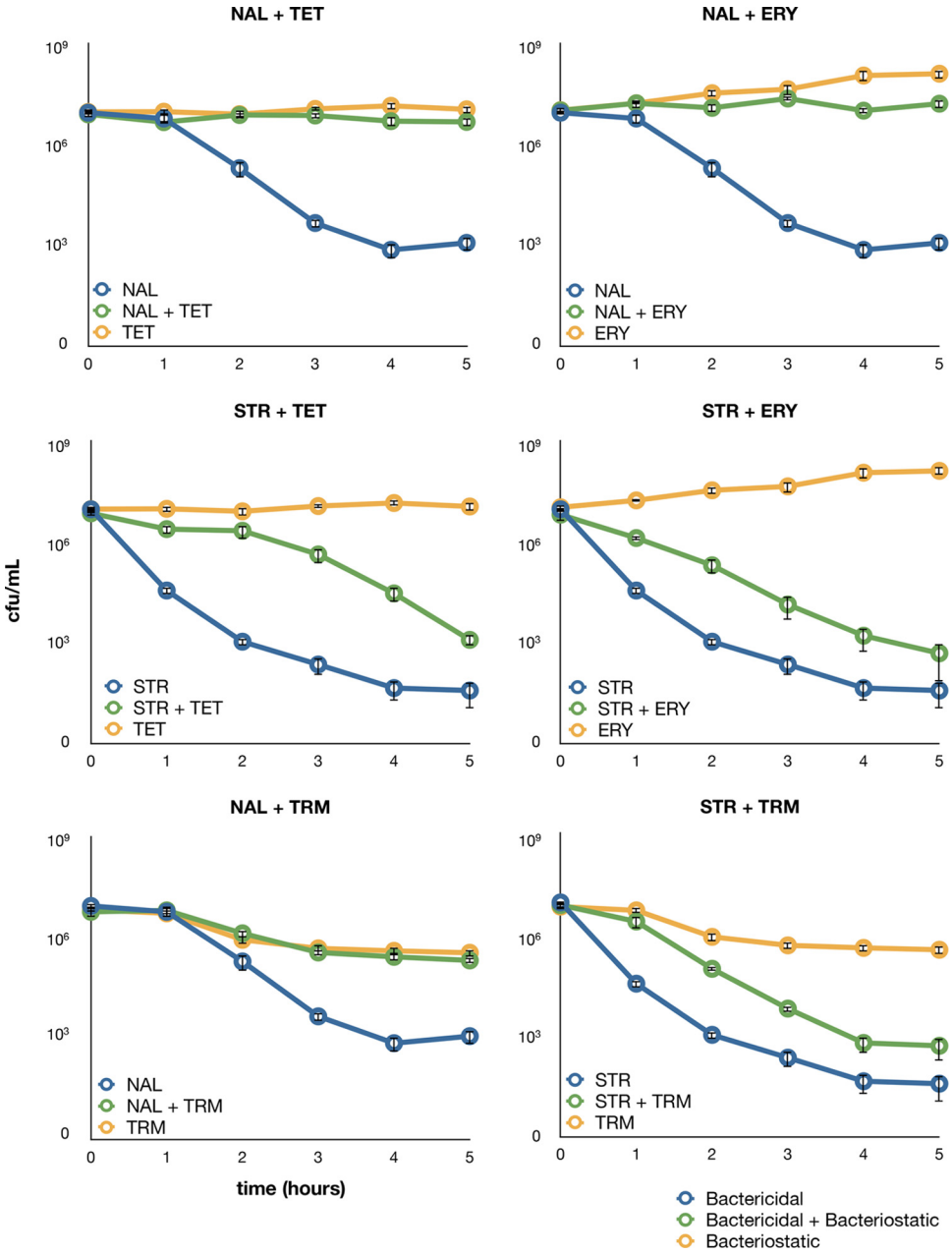

FIG 1 Time-kill curves for single-drug and two-drug combinations. Each graph shows the time-kill curve for a bactericidal-bacteriostatic drug pair and the constituent individual drugs. Error bars represent standard errors of the mean (based on 3 independent replicates) for the number of culturable cells, as measured in CFU/ml at each time point. Antibiotic concentrations used were 25 μg/ml nalidixic acid (NAL), 25 μg/ml streptomycin (STR), 12.5 μg/ml tetracycline (TET), 200 μg/ml erythromycin (ERY), and 10 μg/ml trimethoprim (TRM).

result held after exclusion of antibiotic pairs with overlapping cellular targets ($P = 0.0059$). Thus, our data suggest that bacteriostatic agents antagonize the actions of antibiotics that act on growing cells. This finding is broadly consistent with earlier reports demonstrating that growth inhibition via nutrient limitation often diminishes the effects of bactericidal compounds (35, 36).

Comparison of Fig. 1 and 2 also reveals that antagonistic drug interactions observed beyond the MIC levels are not always apparent at subinhibitory concentrations. Future studies should explore systematically the mechanisms underlying such differences in drug interactions.

Single-drug and combination therapy from the perspective of single cells. Our hypothesis, namely, that bacteriostatic drugs antagonize bactericidal drugs, is independent of the individual molecular mechanisms of action of the drugs but is reliant on the effects of antibiotics on the growth dynamics of single cells. Therefore, we replicated the conditions of our time-kill curves in a microfluidic device, with the goal of directly observing the effects of different antagonistic drug pairs on single cells. We focused on understanding the differences in the effects on cell elongation and division of two bacteriostatic drugs that bind to different ribosomal targets, i.e., erythromycin and tetracycline, with the bactericidal drug nalidixic acid.

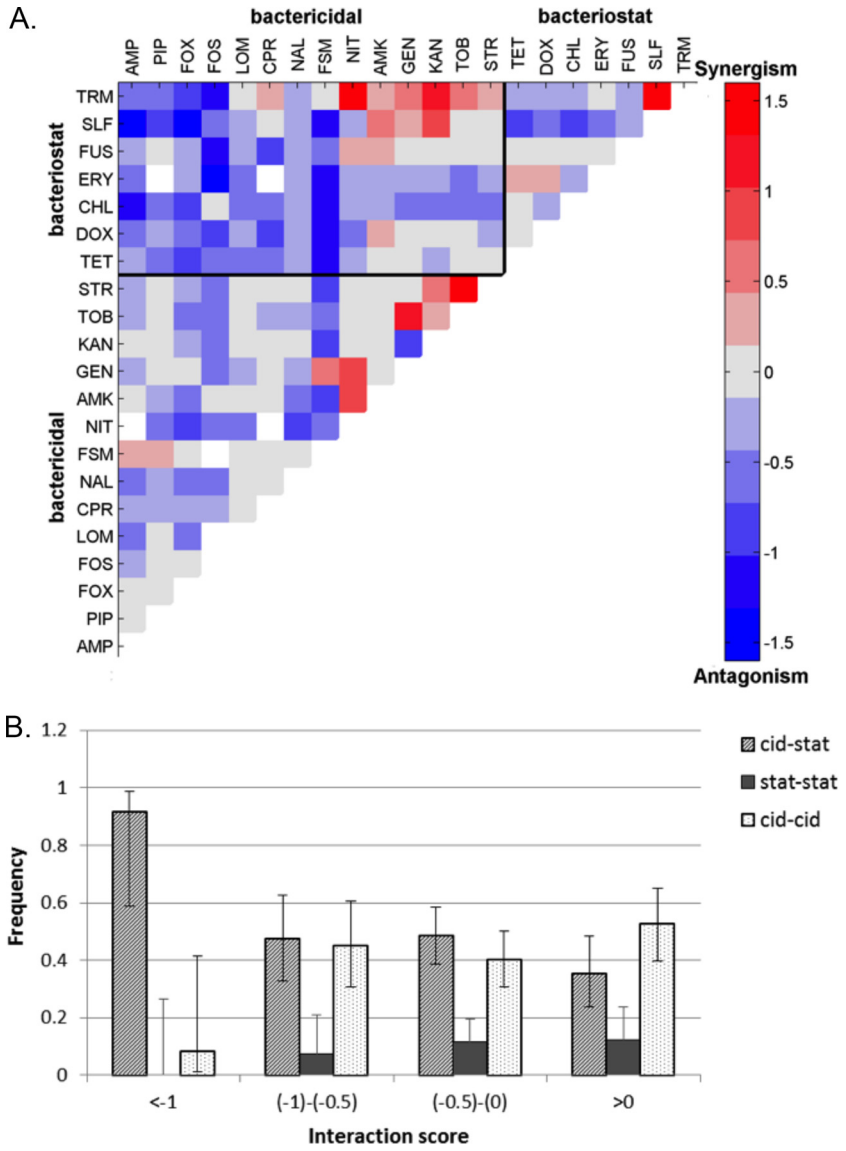

FIG 2 Systematic exploration of interactions between bactericidal and bacteriostatic antibiotics at subinhibitory concentrations. (A) Heatmap showing pairwise interactions between 21 antibiotics measured systematically in *E. coli*. Antibiotics are grouped according to their modes of action, and colors reflect interaction scores. Negative and positive scores correspond to antagonism (blue) and synergism (red), respectively, according to Loewe additivity criteria. White, missing data. For antibiotic abbreviations and concentrations, see Table 1. (B) Graph showing that the combination of a bacteriostatic (stat) antibiotic with a bactericidal (cid) antibiotic has a tendency to show strong antagonism. Antibiotic pairs were categorized according to their individual antibiotic killing properties, leading to three major groups, i.e., bactericidal-bacteriostatic, bacteriostatic-bacteriostatic, and bactericidal-bactericidal. Antibiotic pairs with interaction scores (*B*) lower than −1 (i.e., those showing strong antagonism) were significantly more likely to fall in the bactericidal-bacteriostatic category than were the rest of the antibiotic pairs ($P = 0.0016$, Fisher's exact test).

FIG 3 Length-time graphs for individual cells before, during, and after antibiotic exposure. At least 20 individual cells per antibiotic treatment were selected for analysis using custom software; the results of each treatment were collated in one graph, with each line representing the length of a single cell over time. Upward deflections of these lines denote increases in length, and abrupt downward deflections indicate division events. The shaded section in each graph denotes the period during which antibiotic-containing medium was used. Lines that end abruptly indicate lysis of the cell under observation. The analysis of a population subjected to erythromycin alone was problematic due to the formation of long filamentous cells that were drawn out of their growth channels as medium flowed through the primary trench of the device; this reduced the number of cells available for observation for the entire experiment. Furthermore, in the erythromycin panel, the large fluctuations in cell length indicate the increased size to which these cells were observed to grow, as well as the continuation of division events. The antibiotic concentrations used were 25 μg/ml nalidixic acid, 25 μg/ml streptomycin, 12.5 μg/ml tetracycline, 200 μg/ml erythromycin, and 10 μg/ml trimethoprim. (A) Cells treated with the bactericidal drug nalidixic acid either were lysed or were never found to resume division even after the medium had been changed to drug-free broth. (B) Tetracycline was observed to reduce elongation and completely prevent division during antibiotic exposure, while erythromycin only reduced division rates; this resulted in filamentous cells that were still capable of division, albeit at lower rates than cells grown in drug-free broth. (C) The combination of nalidixic acid and tetracycline produced growth dynamics similar to those observed with tetracycline alone. Erythromycin and nalidixic acid, however, induced filamentation and significantly reduced division. Both conditions resulted in large numbers of cells that were found to resume growth upon a return to drug-free broth.

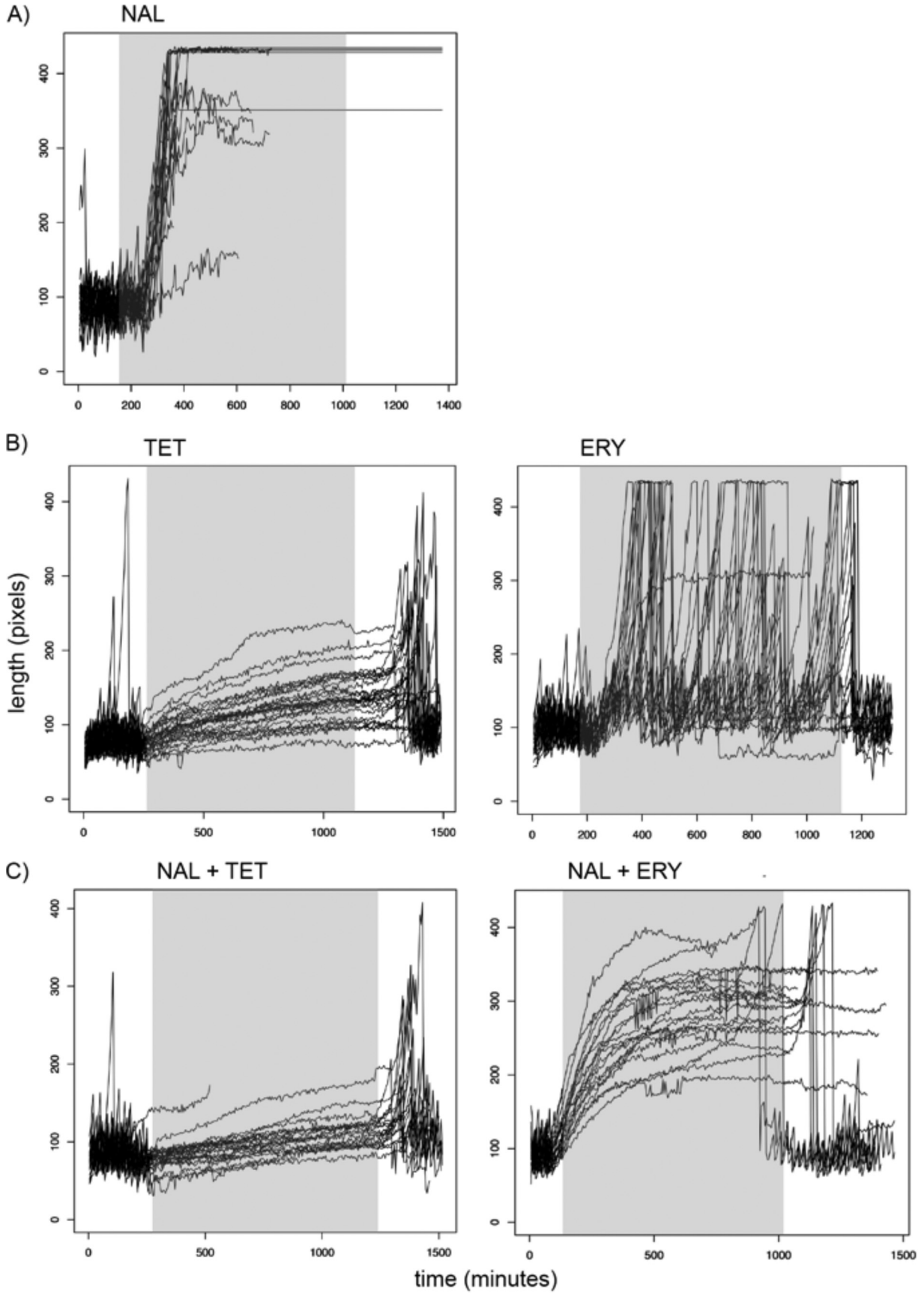
A)
NAL
B)
TET
ERY
length (pixels)
C)
NAL + TET
NAL + ERY
time (minutes)

Using a device designed to track the elongation and division of hundreds of individual cells over a long period (32), we began by growing *E. coli* cells in rich medium without antibiotics for at least 4 h, to determine the baseline rates of these cellular processes. This was followed by exposure to a single drug or pairs of drugs for at least 16 h. Media were then switched back to drug-free broth for at least four more hours.

By analyzing the resulting time-lapse images, we captured quantitative information on the rates of cell elongation and division of single cells as they were subjected to different antibiotics singly or in antagonistic pairs. Furthermore, we monitored the fates of hundreds of cells from every condition to assess viability after withdrawal of antibiotic-containing media. While every cell exposed to bactericidal drugs either was lysed or did not resume growth by the end of the experiment, at least 30% and up to more than 80% of individual cells treated with bactericidal-bacteriostatic drug pairs maintained cellular integrity and resumed division after replacement of antibiotic-free medium (see Table S1 in the supplemental material).

We selected at least 20 individual cells per condition for detailed analysis using custom software. We measured each individual cell's elongation rate, number of cell length doublings per hour, and division rate (number of divisions per hour). Figure 3 depicts the lengths of cells for each condition across the entire duration of the experiment. The graphs reveal qualitative differences in cellular responses to different antibiotic treatments. Our time-lapse images revealed contrasting responses to the bacteriostatic drugs tetracycline and erythromycin. As reported previously, we found that tetracycline exposure reduced cell elongation and decreased the rate of cell division (24). Erythromycin, however, reduced only the rate of division, resulting in filamentous cells that continued to divide. The maximum length depicted in our plots was constrained by the length of the growth channel in the microfluidic device, and we were thus unable to measure the actual size of antibiotic-induced filaments.

To determine whether the strong reductions in elongation and division observed with tetracycline could similarly antagonize another bactericidal antibiotic with an unrelated mechanism of action, we also combined tetracycline with the bactericidal antibiotic streptomycin and repeated the analysis. The resulting growth dynamics are depicted in Fig. S1 in the supplemental material.

In addition to tracking the rates of elongation of cells in the selected conditions, we extracted the rates of division of individual cells as they were subjected to different antibiotic-containing media. In Fig. 4, we present the distributions of the division rates and elongation rates (as cell length doublings per hour) for each population during the period of exposure to antibiotics. Stasis in cell division and elongation was observed for individual cells exposed to the bacteriostatic antibiotic tetracycline. In contrast, treatment with the bacteriostatic drug erythromycin resulted in decreased elongation rates and reduced but not completely restricted division rates. This produced filamentous cells that were still able to divide, albeit at lower rates than cells grown in the absence of drug.

The differences in cellular responses observed in the study of cells exposed to bacteriostatic drugs extended to the results for antagonistic drug pairs. Cells treated with tetracycline and either of the bactericidal drugs demonstrated greatly reduced growth rates and ceased dividing until the antibiotics were withdrawn, while erythromycin paired with a bactericidal drug halted cell division, resulting in long filamentous cells that proceeded with division only after replacement of drug-free medium. Our time-lapse microscopy experiments thus revealed contrasting responses of bacteria exposed to drugs belonging to the same pharmacodynamic class. These differing responses extended to treatment with different antagonistic drug pairs.

DISCUSSION

The relevance of classifying antibiotics as bacteriostatic or bactericidal has been questioned due to the reliance of these categories on drug concentrations and the treated organisms (37). The manner in which these pharmacodynamic properties are used in specific clinical scenarios is beyond the scope of this paper. Instead, we propose that this binary classification is a useful initial step in determining when two drugs in combination would result in strong antagonism and thus should be evaluated, to exploit the varied effects of this specific interaction.

The tests set by the Clinical and Laboratory Standards Institute (31) to determine whether an antibiotic is bacteriostatic or bactericidal involve assessing the degree of survival of a liquid culture of bacteria after a certain period of drug exposure. The moderate killing effect that defines a bacteriostatic agent therefore implies induction of cellular stasis. Here we show that, while bacteriostatic drugs result in prevalent patterns of antagonistic interactions with bactericidal drugs, their effects at the single-cell level may differ considerably. We found that tetracycline effectively induced stasis in antibiotic-sensitive bacteria. In contrast, treatment with erythromycin reduced the elongation rate to a similar degree as did tetracycline, while division rates were not as strongly decreased; this resulted in long filamentous cells.

The disparities in growth dynamics with similarly antagonistic antibiotic combinations (Fig. 3C) suggest that different cellular mechanisms underlie the increased survival rates with these pairs of drugs. However, the results of our time-lapse image analysis suggest a new perspective on how and when cells can elude killing by antibiotics. This method allowed for the examination of cell growth as distinct rates of elongation and division (Fig. 4). The similar reductions in division rates produced by different bacteriostatic-bactericidal drug pairs could be the basis of antagonism. In relation to the morphological effects we quantified, other antibiotics are capable of eliciting changes in cell shape. For example, members of the beta-lactam class induce cell lysis via a bulge-mediated process in which the cytosol leaks out through defects produced in the peptidoglycan layer (38). Future work should consider whether such structural effects are capable of modulating rates of cell division and therefore would be similarly capable of producing antagonism.

In a complementary study, a separate element of bacterial physiology has been found to be important in killing by antibiotics. Allison and colleagues distinguished metabolic activity from growth as a factor that potentiates the killing of dormant cells by aminoglycosides (39). Determining conditions that affect specific aspects of cell physiology, such as increasing metabolic activity or inhibiting division, could be important for designing new antibiotics or increasing the efficiency of our currently available drugs.

Our results urge caution before forming general assumptions regarding the effects of drug interactions. Although our studies of bacteriostatic and bactericidal drugs reveal pervasive antagonism in growth and death rates, the variety of morphological responses we observe may lead to antibiotic combination-specific fitness effects. Furthermore, the bacteriostatic/bactericidal classification

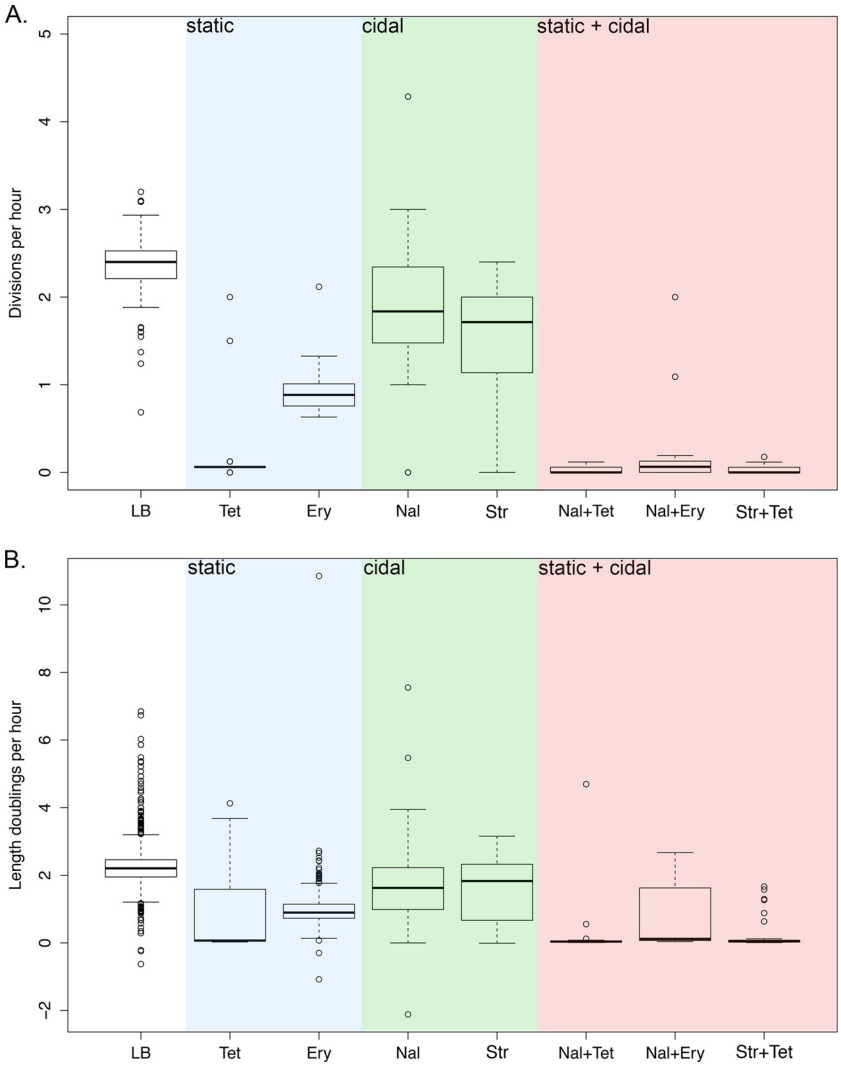

FIG 4 Effects of single and paired antibiotics on cell division and elongation. We extracted the rates of division (A) and elongation (cell length doublings per hour) (B) from each of the individual cells included in our detailed analysis, and we present the distribution of these rates as box plots. Rates for the antibiotic-free LB broth condition were calculated by pooling the division and elongation rates for every individual cell across all conditions prior to drug exposure. Negative elongation rates are from filamentous cells that divide several times without elongation between division events. The boxes span the range between the upper and lower quartiles. Thick lines, medians; whiskers, highest and lowest values still within 1.5 interquartile ranges of the upper and lower quartiles, respectively; ○, data points outside this range.

system varies across organisms and even across drug concentrations, and the interactions between drugs may similarly shift. Assessing *in vitro* drug interactions across a wide range of concentrations can guide *in vivo* studies, where variables such as absorption rates, elimination rates, and dosing regimens may lead to fluctuations in concentrations (6). Additionally, other variables intrinsic to the *in vivo* environment, such as changes in pH across body compartments, may result in changes to drug interactions that cannot be predicted in *in vitro* experiments.

Antibiotic combination therapy remains an important option as a treatment strategy aimed at controlling the rise of resistance. As this goal is approached, the single-cell dynamics we observed with different antagonistic drug pairs indicate that closer examination of the effects of antibiotics on individual components of bacterial physiology would aid in our understanding and utilization of drug combinations for more bacterial infections.

ACKNOWLEDGMENTS

We thank Ima Avalos Vizcarra for help with microfluidics and Rafael Pena-Miller and Rob Beardmore for developing the image analysis software we employed.

V.L., B.P., and C.P. thank the Wellcome Trust, the Lendulet program of the Hungarian Academy of Sciences, and the European Research Council for their support. S.B. was supported by the European Research Council under the 7th Framework Programme of the European Commission (grant agreement 268540). P.A.Z.W. received funding from the Swiss National Science Foundation and the German Academic Exchange Service. M. Arnoldini and M. Ackermann received funding from the Swiss National Science Foundation.

REFERENCES

1. **Bonhoeffer S, Lipsitch M, Levin BR.** 1997. Evaluating treatment protocols to prevent antibiotic resistance. Proc. Natl. Acad. Sci. U. S. A. **94:** 12106–12111. http://dx.doi.org/10.1073/pnas.94.22.12106.

2. **Hand K.** 2006. Tuberculosis: pharmacological management. Hosp. Pharm. **13:**81–85.
3. **Mocroft A, Vella S, Benfield TL, Chiesi A, Miller V, Gargalianos P, d'Arminio Monforte A, Yust I, Bruun JN, Phillips AN, Lundgren JD, EuroSIDA Study Group.** 1998. Changing patterns of mortality across Europe in patients infected with HIV-1. Lancet **352:**1725–1730. http://dx.doi.org/10.1016/S0140-6736(98)03201-2.
4. **WHO.** 2010. WHO guidelines for the treatment of malaria, 2nd ed. WHO, Geneva, Switzerland.
5. **Gilbert DN, Moellering RC, Eliopoulos GM, Chambers HF, Saag MS (ed).** 2010. The Sanford guide to antimicrobial therapy, 40th ed. Antimicrobial Therapy, Inc., Sperryville, VA.
6. **Cottarel G, Wierzbowski J.** 2007. Combination drugs, an emerging option for antibacterial therapy. Trends Biotechnol. **25:**547–555. http://dx.doi.org/10.1016/j.tibtech.2007.09.004.
7. **Forrest GN, Tamura K.** 2010. Rifampin combination therapy for nonmycobacterial infections. Clin. Microbiol. Rev. **23:**14–34. http://dx.doi.org/10.1128/CMR.00034-09.
8. **Cunha BA.** 2004. Therapeutic implications of antibacterial resistance in community-acquired respiratory tract infections in children. Infection **32:**98–108. http://dx.doi.org/10.1007/s15010-004-3065-5.
9. **Ankomah P, Johnson PJT, Levin BR.** 2013. The pharmaco –, population and evolutionary dynamics of multi-drug therapy: experiments with *S. aureus* and *E. coli* and computer simulations. PLoS Pathog. **9:**e1003300. http://dx.doi.org/10.1371/journal.ppat.1003300.
10. **Johansen HK, Jensen TG, Dessau RB, Lundgren B, Frimodt-Moller N.** 2000. Antagonism between penicillin and erythromycin against *Streptococcus pneumoniae* in vitro and in vivo. J. Antimicrob. Chemother. **46:**973–980. http://dx.doi.org/10.1093/jac/46.6.973.
11. **Cates JE, Christie RV, Garrod LP.** 1951. Penicillin-resistant subacute bacterial endocarditis treated by a combination of penicillin and streptomycin. Br. Med. J. **1:**653–656.
12. **Garrod L.** 1972. Causes of failure in antibiotic treatment. Br. Med. J. **4:**473–476. http://dx.doi.org/10.1136/bmj.4.5838.473.
13. **Yeh PJ, Hegreness MJ, Aiden AP, Kishony R.** 2009. Drug interactions and the evolution of antibiotic resistance. Nat. Rev. Microbiol. **7:**460–466. http://dx.doi.org/10.1038/nrmicro2133.
14. **Chait R, Craney A, Kishony R.** 2007. Antibiotic interactions that select against resistance. Nature **446:**668–671. http://dx.doi.org/10.1038/nature05685.
15. **Hegreness M, Shoresh N, Damian D, Hartl D, Kishony R.** 2008. Accelerated evolution of resistance in multidrug environments. Proc. Natl. Acad. Sci. U. S. A. **105:**13977–13981. http://dx.doi.org/10.1073/pnas.0805965105.
16. **Nitzan O, Supornitzky U, Kennes Y, Chazan B, Raz R, Colodner R.** 2010. Is chloramphenicol making a comeback? Isr. Med. Assoc. J. **12:**371–374.
17. **Falagas ME, Grammatikos AP, Michalopoulos A.** 2008. Potential of old-generation antibiotics to address current need for new antibiotics. Expert Rev. Anti Infect. Ther. **6:**593–600. http://dx.doi.org/10.1586/14787210.6.5.593.
18. **Wilson G, Miles A.** 1964. Topley and Wilson's principles of bacteriology and immunity, 5th ed. Edward Arnold, London, United Kingdom.
19. **Jawetz E, Gunnison J.** 1953. Antibiotic synergism and antagonism: an assessment of the problem. Pharmacol. Rev. **5:**175–192.
20. **Jawetz E, Gunnison J, Coleman VR.** 1954. Observations on the mode of action of antibiotic synergism and antagonism. J. Gen. Microbiol. **10:**191–198. http://dx.doi.org/10.1099/00221287-10-2-191.
21. **Lázár V, Pal Singh G, Spohn R, Nagy I, Horváth B, Hrtyan M, Busa-Fekete R, Bogos B, Méhi O, Csörgő B, Pósfai G, Fekete G, Szappanos B, Kégl B, Papp B, Pál C.** 2013. Bacterial evolution of antibiotic hypersensitivity. Mol. Syst. Biol. **9:**700. http://dx.doi.org/10.1038/msb.2013.57.
22. **Yeh P, Tschumi AI, Kishony R.** 2006. Functional classification of drugs by properties of their pairwise interactions. Nat. Genet. **38:**489–494. http://dx.doi.org/10.1038/ng1755.
23. **Warringer J, Blomberg A.** 2003. Automated screening in environmental arrays allows analysis of quantitative phenotypic profiles in *Saccharomyces cerevisiae*. Yeast **20:**53–67. http://dx.doi.org/10.1002/yea.931.
24. **Rasmussen CE, Williams CKI.** 2006. Gaussian processes for machine learning. MIT Press, Cambridge, MA.
25. **Drusano GL, D'Argenio DZ, Preston SL, Barone C, Symonds W, LaFon S, Rogers M, Prince W, Bye A, Bilello JA.** 2000. Use of drug effect interaction modeling with Monte Carlo simulation to examine the impact of dosing interval on the projected antiviral activity of the combination of abacavir and amprenavir. Antimicrob. Agents Chemother. **44:**1655–1659. http://dx.doi.org/10.1128/AAC.44.6.1655-1659.2000.
26. **Drusano GL, D'Argenio DZ, Symonds W, Bilello PA, McDowell J, Sadler B, Bye A, Bilello JA.** 1998. Nucleoside analog 1592U89 and human immunodeficiency virus protease inhibitor 141W94 are synergistic in vitro. Antimicrob. Agents Chemother. **42:**2153–2159.
27. **Greco WR, Bravo G, Parsons JC.** 1995. The search for synergy: a critical review from a response surface perspective. Pharmacol. Rev. **47:**331–385.
28. **Loewe S.** 1953. The problem of synergism and antagonism of combined drugs. Arzneimittelforschung **3:**285–290.
29. **Cokol M, Chua HN, Tasan M, Mutlu B, Weinstein ZB, Suzuki Y, Nergiz ME, Costanzo M, Baryshnikova A, Giaever G, Nislow C, Myers CL, Andrews BJ, Boone C, Roth FP.** 2011. Systematic exploration of synergistic drug pairs. Mol. Syst. Biol. **7:**544. http://dx.doi.org/10.1038/msb.2011.71.
30. **Lehar J, Zimmerman GR, Krueger AS, Molnar RA, Ledell JT, Heilbut AM, Short GF, III, Giusti LC, Nolan GP, Magid OA, Lee MS, Borisy AA, Stockwell BR, Keith CT.** 2007. Chemical combination effects predict connectivity in biological systems. Mol. Syst. Biol. **3:**80. http://dx.doi.org/10.1038/msb4100116.
31. **Clinical and Laboratory Standards Institute.** 2006. Methods for dilution antimicrobial susceptibility tests for bacteria that grow aerobically; approved standard—7th ed. Clinical and Laboratory Standards Institute, Wayne, PA.
32. **Wang P, Robert L, Pelletier J, Dang WL, Taddei F, Wright A, Jun S.** 2010. Robust growth of *Escherichia coli*. Curr. Biol. **20:**1099–1103. http://dx.doi.org/10.1016/j.cub.2010.04.045.
33. **Loewe S.** 1928. Die quantitiven Probleme der Pharmakologie. Ergeb. Physiol. **27:**47–187. http://dx.doi.org/10.1007/BF02322290.
34. **Bollenbach T, Quan S, Chait R, Kishony R.** 2009. Nonoptimal microbial response to antibiotics underlies suppressive drug interactions. Cell **139:**707–718. http://dx.doi.org/10.1016/j.cell.2009.10.025.
35. **Cozens RM, Tuomanen E, Tosch W, Zak O, Suter J, Tomasz A.** 1986. Evaluation of the bactericidal activity of β-lactam antibiotics on slowly growing bacteria cultured in the chemostat. Antimicrob. Agents Chemother. **29:**797–802. http://dx.doi.org/10.1128/AAC.29.5.797.
36. **Eng RHK, Padberg FT, Smith SM, Tan EN, Cherubin CE.** 1991. Bactericidal effects of antibiotics on slowly growing and nongrowing bacteria. Antimicrob. Agents Chemother. **35:**1824–1828. http://dx.doi.org/10.1128/AAC.35.9.1824.
37. **Pankey G, Sabath L.** 2004. Clinical relevance of bacteriostatic versus bactericidal mechanisms of action in the treatment of Gram-positive bacterial infections. Clin. Infect. Dis. **38:**864–870. http://dx.doi.org/10.1086/381972.
38. **Yao Z, Kahne D, Kishony R.** 2012. Distinct single-cell morphological dynamics under β-lactam antibiotics. Mol. Cell **48:**705–712. http://dx.doi.org/10.1016/j.molcel.2012.09.016.
39. **Allison K, Brynildsen M, Collins J.** 2011. Metabolite-enabled eradication of bacterial persisters by aminoglycosides. Nature **473:**216–220. http://dx.doi.org/10.1038/nature10069.